JOURNAL OF SOLID STATE CHEMISTRY 76, 301–312 (1988)

Defects in β-Rhombohedral Boron Formed during the Synthesis of LaB_6

PER-OLOF OLSSON

Department of Inorganic Chemistry, Arrhenius Laboratory, University of Stockholm, S-106 91 Stockholm, Sweden

Received November 10, 1987; in revised form April 29, 1988

Beta-rhombohedral boron (a = 10.139 Å, α = 65.20°, Z = 104.9, space group $R\bar{3}m$), formed during the synthesis of LaB_6 has been investigated with the use of high-resolution electron microscopy. In a sample of gross composition $La_{0.81}B_6$, β-rhombohedral boron crystals were found. Microanalysis showed that some of these contained minor amounts of La, Si, and O. They were rich in defects of various kinds, such as point defects, line defects, stacking faults, and twinning. Structure models are suggested for some of the defects. © 1988 Academic Press, Inc.

Introduction

The existence of a homogeneity range for lanthanum hexaboride has been established, but the exact limits are not known. This is partly due to the difficulties in detecting small amounts of boron in mixtures with LaB_6 as a consequence of the unfavorable ratio of the X-ray scattering factors and the tendency of boron to occur in amorphous or heavily twinned form (*1*).

In a search for extra phases a sample of the nominal composition $La_{0.81}B_6$, which only exhibited the X-ray powder pattern of cubic LaB_6, was investigated by high-resolution electron microscopy (HREM). In this sample crystals with the β-rhombohedral boron structure were found, and these were unusually rich in defects.

Defects in β-boron have been reported by several investigators using various kinds of electron-optical techniques (*2–5*). McKelvy *et al.* (*6*) were the first to use HREM and they gave a plausible structure model for twinning across {100}. In the present paper the results of our HREM investigation of the β-boron crystals are presented. New types of defects are observed, and plausible models for these are presented and verified by image simulations.

The Crystal Structure

The first determination of the rather complicated crystal structure of β-rhombohedral boron was made by Hughes *et al.* (*7*) with subsequent refinements by several other groups (*8–10*). The structure has the unit cell dimensions: a = 10.139 Å, α = 65.20°; the space group is $R\bar{3}m$ and the cell contains 104.9 atoms, the nonintegral number being due to fractional occupancy of two sites. The structure (potential) projected along [001] and [1$\bar{1}$0] is shown in Fig. 1, with part of the atomic arrangement indicated. The structure can be described in terms of icosahedra or half-icosahedra.

One icosahedron, $B12_c$ in Fig. 1, is cen-

0022-4596/88 $3.00

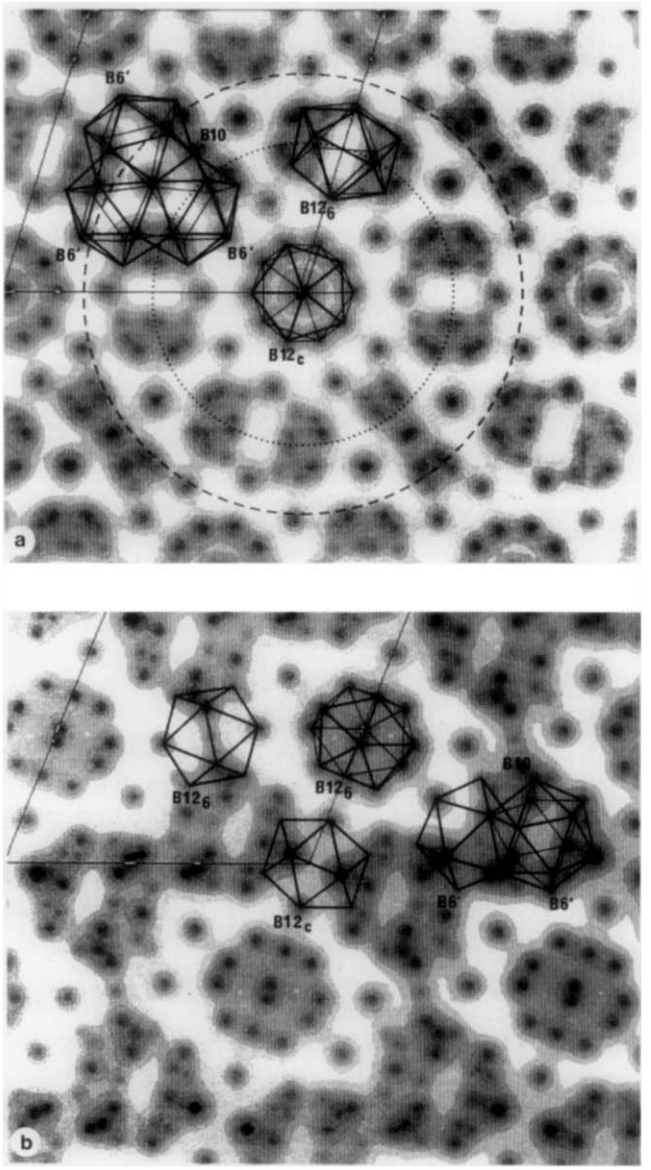

FIG. 1. (a) Projected potential of the structure of β-rhombohedral boron in the $\langle 001 \rangle$ directions. The axes of the indicated unit cell are the projections of the a- and b-axes. The central icosahedron $B12_c$, one $B12_6$ icosahedron formed by two B6 units, and one B10 unit connected to three B6′ units are indicated. Note that $B12_6$ icosahedra also project on top of the $B12_6$ icosahedra. Also indicated are one B_{84} unit (dotted circle) and one B_{156} unit (dashed circle). (b) Projected potential of the lattice in the $\langle 1\bar{1}0 \rangle$ directions. The axes of the indicated unit cell are the projections of the c-axis and the [110] vector. The central icosahedron $B12_c$, two $B12_6$ icosahedrons, and a complex consisting of a B10 unit connected to three B6′ units are indicated. Note that two of the three B6′ units coincide in this projection.

tered at the origin of the unit cell. It is surrounded by 12 half-icosahedra thus forming spherical clusters containing 84 atoms (B_{84}). Six of these half-icosahedra (B6) extended in the ⟨100⟩ directions and meet equivalent B6 units to form complete icosahedra ($B12_6$). The other six half-icosahedra (B6′) are found in the ⟨110⟩ directions, and each is connected to a B10 unit. This unit, in turn, can be regarded as composed of three half-icosahedra sharing faces, and since it is capped by half-icosahedra in three directions, a cluster of three independent icosahedra forms. There is one additional boron atom at the center of the cell, and finally there is one interstitial site with relatively low occupancy outside the central icosahedron, close to the threefold axis.

Experimental

The sample investigated by HREM had been prepared by Dr. Yu. B. Paderno, Kiev, using the boro-thermal reduction reaction (*11*). The nominal composition prepared was $La_{0.81}B_6$. The sample was a dark blue microcrystalline powder. For the electron microscopy investigation, the specimens were ground in a mortar, dispersed in butanol, and dried on a holey carbon film. For the HREM studies a Siemens Elmiskop 102 (125 kV, 3.5 Å resolution) and a Jeol 200CX (200 kV, 2.5 Å resolution) were used. Both were equipped with double-tilt stages. The elemental analysis was performed with a dedicated STEM (VG Microscopes HB501) equipped with EDX and EELS. Multislice image calculations were done using a locally modified version of the SHRLI program package (*12*). The axes of projection are long, but the multislice calculations were made using thin (3.3 Å) slices corresponding to different levels of the unit cell. The final matching of calculated and experimental images was done with a Kontron-IPS image processing system. The atomic positions used for the β-boron structure were those given by Callmer (*10*).

Analysis

The bulk chemical analysis of the sample showed that it contained 63.1% La and 36.4% B (*11*). During the TEM analysis of the sample it was found that it contained two dominant phases: LaB_6, and crystals having the β-rhombohedral boron structure, in a proportion larger than 20 to 1. The β-boron cyrstals were almost always found joined to LaB_6 crystals, but no actual intergrowth was noticed. The β-boron crystals were in the form of relatively thin flakes, rather easily distinguished from the thicker LaB_6 crystals. Amorphous fragments were also present.

The EDX analysis of the LaB_6 type crystals showed that they contained only La besides undetectable light elements. The β-boron phase gave indications of minor amounts of lanthanum and silicon. Analyses made with a small probe in different areas of the same crystal showed a slight variation in the intensity, which suggests that it may contain slightly variable amounts of La and Si.

The EELS analysis showed clear La$M_{4,5}$ peaks from some of the β-boron crystals, while others gave no detectable signal. The L_1 edge of Si was also observed in some fragments and seemed always to be associated with an oxygen signal. No silicon signal was recorded with the beam directed onto the LaB_6 crystals. The amorphous material observed was shown to contain essentially silicon and oxygen. Most of the β-boron crystals thus seem to contain small, variable amounts of La and possibly also Si. However, no quantitative microanalysis could be made. At least part of the Si is present as a separate oxide phase. The

FIG. 2. (a) [001] image taken with the Siemens Elmiskop 102. (b) [001] diffraction pattern corresponding to (a). The twinning gives rise to two lattices with a common $h00$ line. The 040 diffraction spots are arrowed.

silicon and oxygen found in the sample probably come from silicon in the starting materials. Since silicon forms a solid solution with boron (*13*) it is possible that some Si may have been incorporated into the boron structure. The structural change thereby produced would be insignificant in the present context, however.

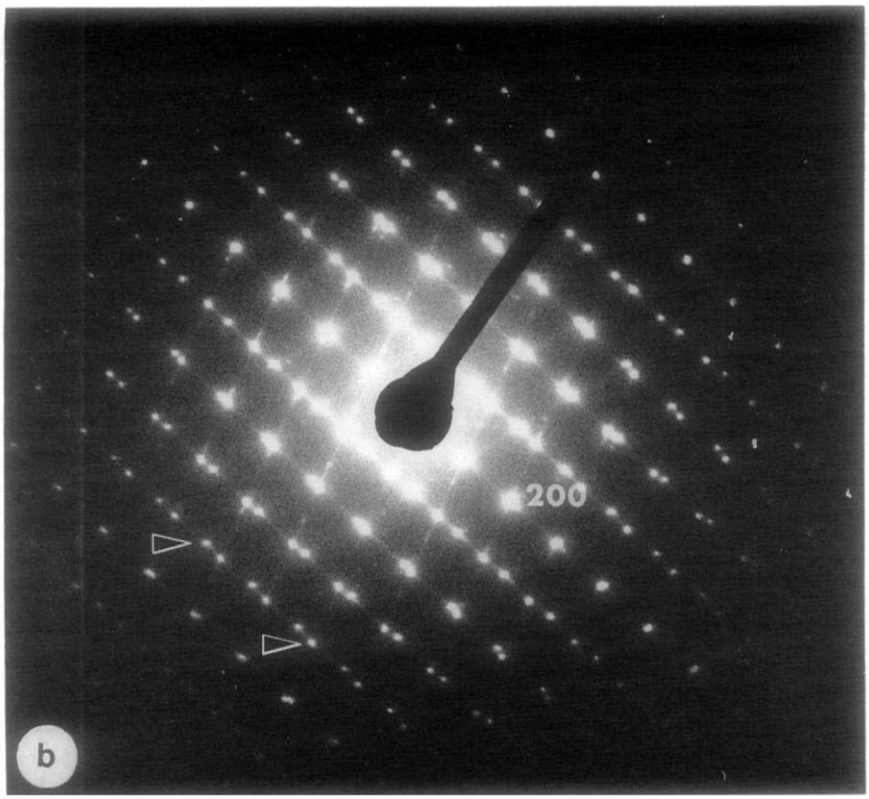

FIG. 2—*Continued.*

Electron Microscopy

The HREM investigations of the β-rhombohedral boron crystals received a large number of defects and an intricate twinning pattern as shown in Figs. 2a and 3. The crystals are seen to consist of domains and are characterized by frequent twinning across {100}. Isolated twin faults of this type have previously been described by McKelvy *et al.* (*6*). The twinning and the different defects are revealed also in the diffraction pattern shown in Fig. 2b. In Fig. 2a the contrast varies between different parts of the micrograph. This is probably due to differences in alignment of the crystal with respect to the beam, due to extensive twinning.

In order to interpret the micrographs, image-calculations based on the β-boron structure (*10*) were made for various defocus and thickness values. A calculated image of the β-rhombohedral boron structure, inserted in a part of Fig. 3a, is shown in Fig. 4.

Fig. 3a, taken along [001], shows essentially three domains marked A, B, and C, each extensively twinned across (100). The domains are separated by borders consisting of plane segments. The A/B border planes are (010) stacking faults or (100) twin interfaces. The B/C border has several parts parallel to $(1\bar{1}0)$, but the two domains are related by the same type of shift, but now in the opposite direction. The combination of these twin-planes in several directions gives rise to interactions for which structure models can be proposed. The

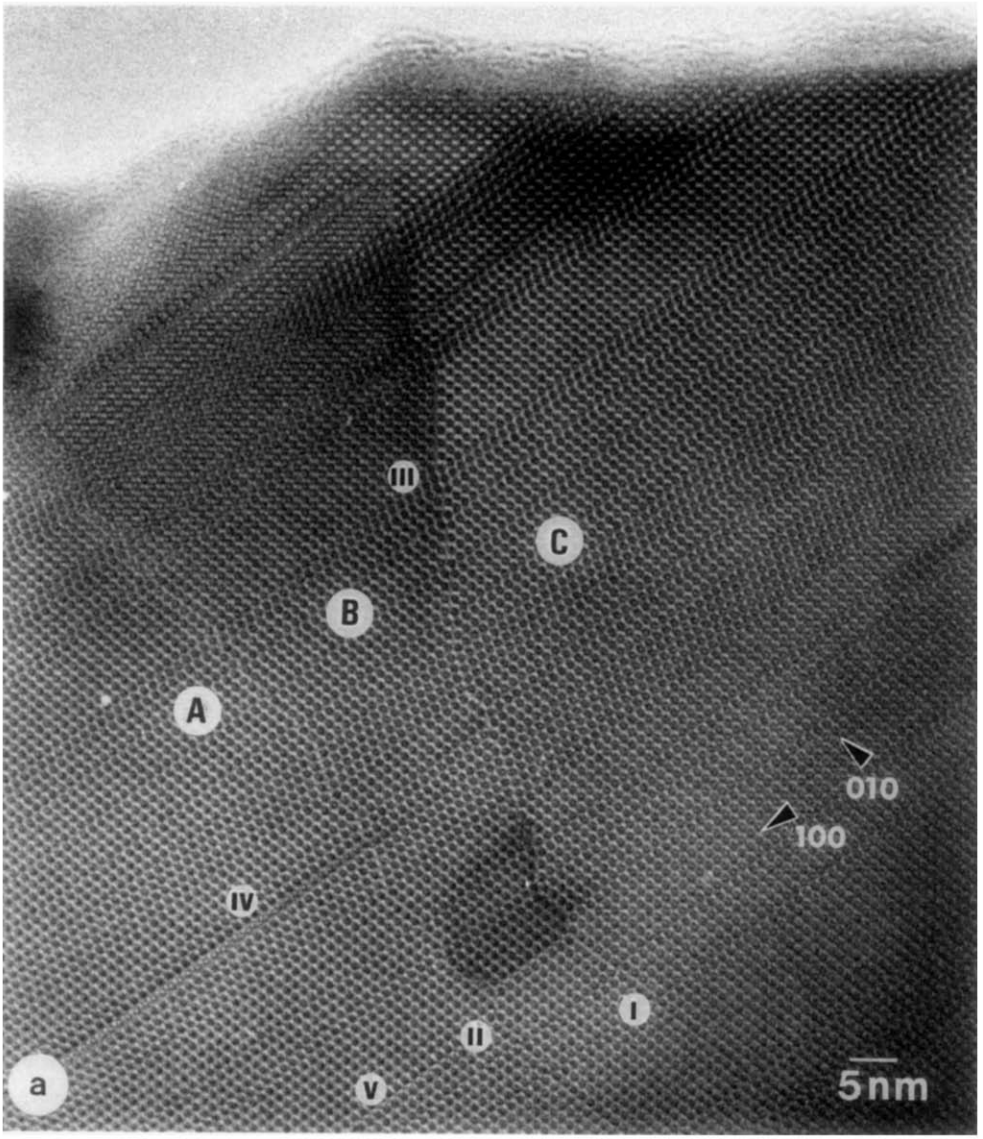

FIG. 3. (a) [001] image taken with the Siemens Elmiskop 102. Indicated are five types of defects: (I), (II), (III), (IV), and (V). (b) Enlarged parts of (a). The five defects indicated in (a) are shown.

simplest case is the twin cross (marked as I in Fig. 3a). When only complete unit cells are used in the model, a hole of the size of somewhat more than two unit cells is created. It can be partly filled by extending the structure in a regular way toward the center of the defect using complete icosahedral units as shown in Fig. 5. A more detailed defect model cannot be proposed, however, due to the lack of resolution in the image and difficulties in handling the large unit cell necessary for image simulation by the periodic continuation method (*14, 15*).

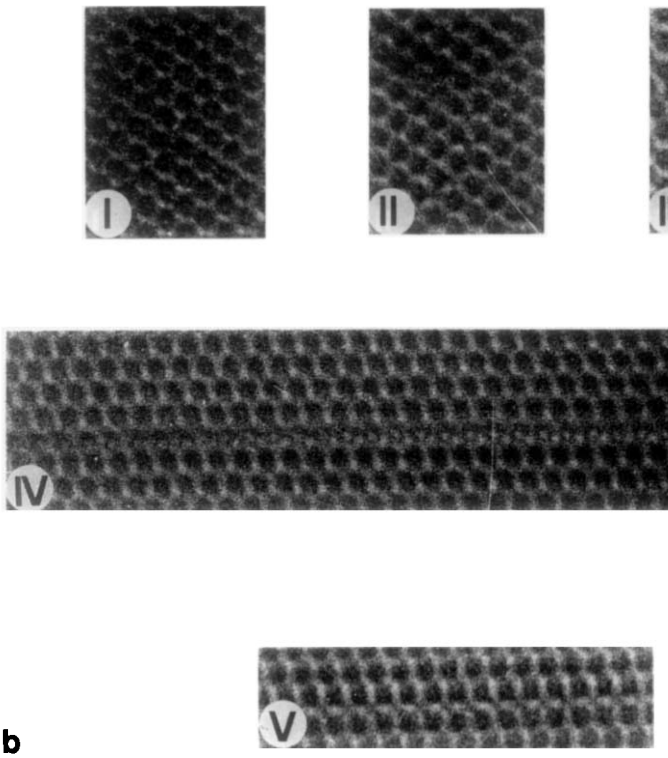

FIG. 3—*Continued.*

Several variations of this defect are also visible in Fig. 3. These include an elongation of the fault (II) to contain eight $B12_c$ units around the cavity instead of six. Several "twin-crosses" can be seen to form an extended defect at the borderline between two areas of extensive twinning (III). Models for the two defects are proposed in Figs. 6 and 7. In all these cases it is possible to extend the structure in a rather normal way toward the center of the defect, in analogy with Fig. 5.

Among the different variations of twinning which can be seen in Fig. 3, there is one implying a gradual change, parallel to the twin plane, from twinned to normal structure (IV) along the [100] direction. This defect is different from the others, as it is obviously not parallel with the zone axis.

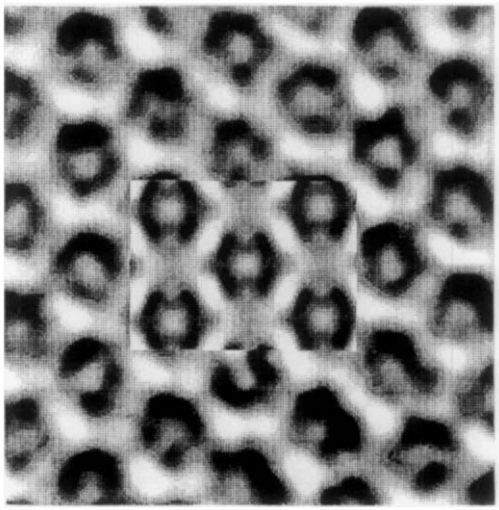

FIG. 4. Enlarged part of Fig. 3a with calculated inserted image. The image was calculated for a thickness of 650 Å and a defocus of −622 Å.

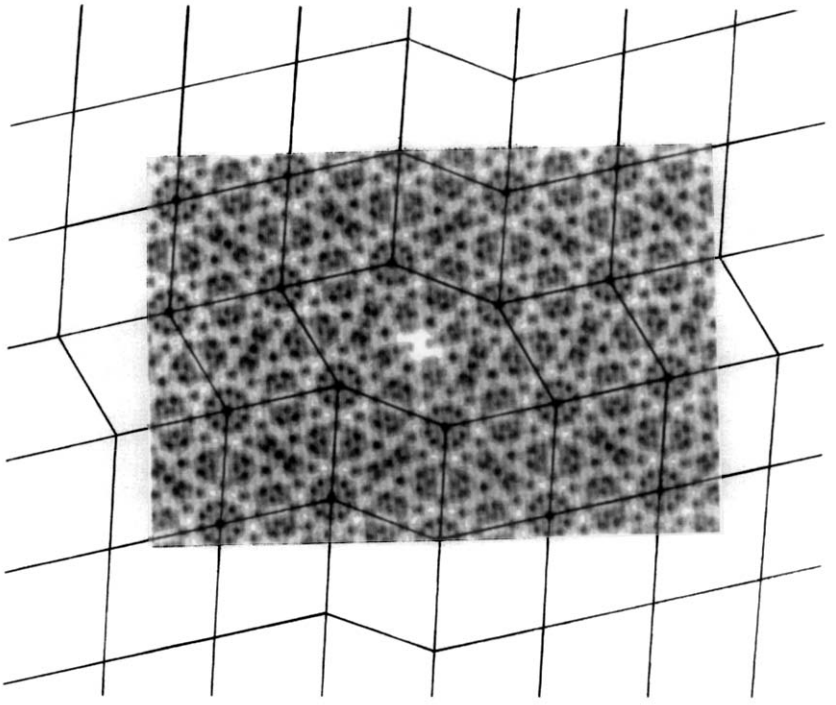

FIG. 5. Projected potential for the "twin-cross." Ordinary unit cells are indicated.

A tentative model of the defect, for one unit cell layer, is given in Fig. 8 and implies a step at a single twinned layer. Thus this defect step appears to be gradually shifted sideways along [100] in successive unit cell layers. The shifted area extends across some 30 unit cells along [100], and this may be taken as an indication that the crystal is at least about 250–300 Å thick in this area.

Figure 9 shows an image taken at higher resolution, parallel with the [1$\bar{1}$0] zone-

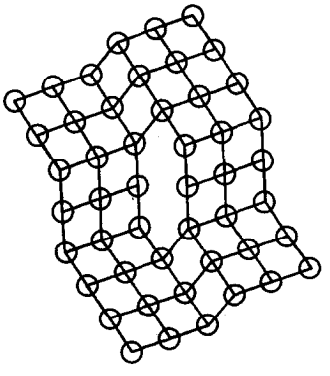

FIG. 6. Model of defect (II). The circles indicate the positions of the central icosahedron ($B12_c$).

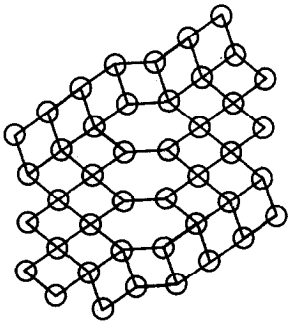

FIG. 7. Model of defect (III). The circles indicate the positions of the central icosahedron ($B12_c$).

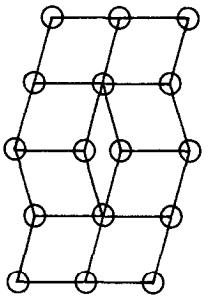

FIG. 8. Tentative model of the "defect unit" for defect (IV). The circles indicate the positions of the central icosahedron ($B12_c$). The four unit cells in the left part of the model represent the left part of the defect. The defect changes gradually along [001] until the structure of the defect matches the right part of the model.

axis. A part of this image, from a thin portion of the crystal, is shown in Fig. 10, with a patch of a calculated image inserted. A fault along [001] is seen in the center of Fig. 9 (arrowed). Across the fault the lattice is shifted by approximately $1/3\ [\bar{1}10]_{proj}-1/2\ [001]_{proj}$. A plausible structure interpretation is given in Fig. 11. It includes one $B12_6$ icosahedron (formed by two B6 half-icosahedra) situated on one side of the defect, bonded to a $B12_{6'}$ icosahedron composed of half-icosahedra originating from a B10 unit and a B6′ unit. This means that the defect is formed by two icosahedra joined by sharing a triangular face. Two such links are created, making the defect centrosymmetric. The calculated image based on this model is inserted in the experimental one in Fig. 12. A defect observed in Fig. 3 (V) can be interpreted as the same type of fault but seen in a different direction, [001]. This was verified by image calculations.

Discussion

The ease with which the different defects seen in Figs. 2 and 3 form in the β-boron

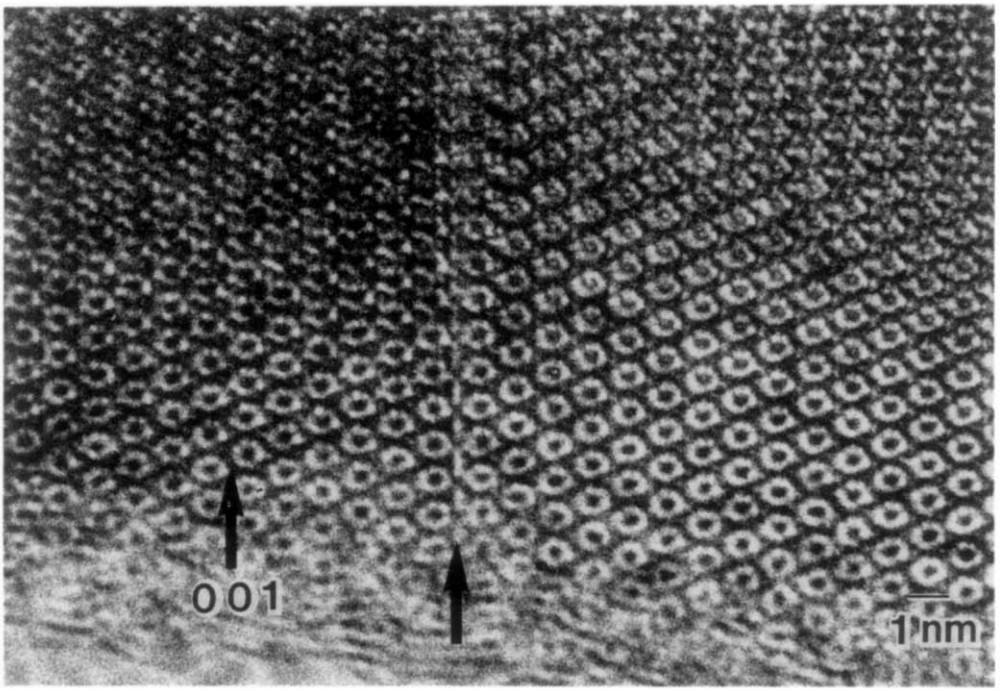

FIG. 9. $[1\bar{1}0]$ image taken with the Jeol 200CX. The [001] direction and a line fault is arrowed.

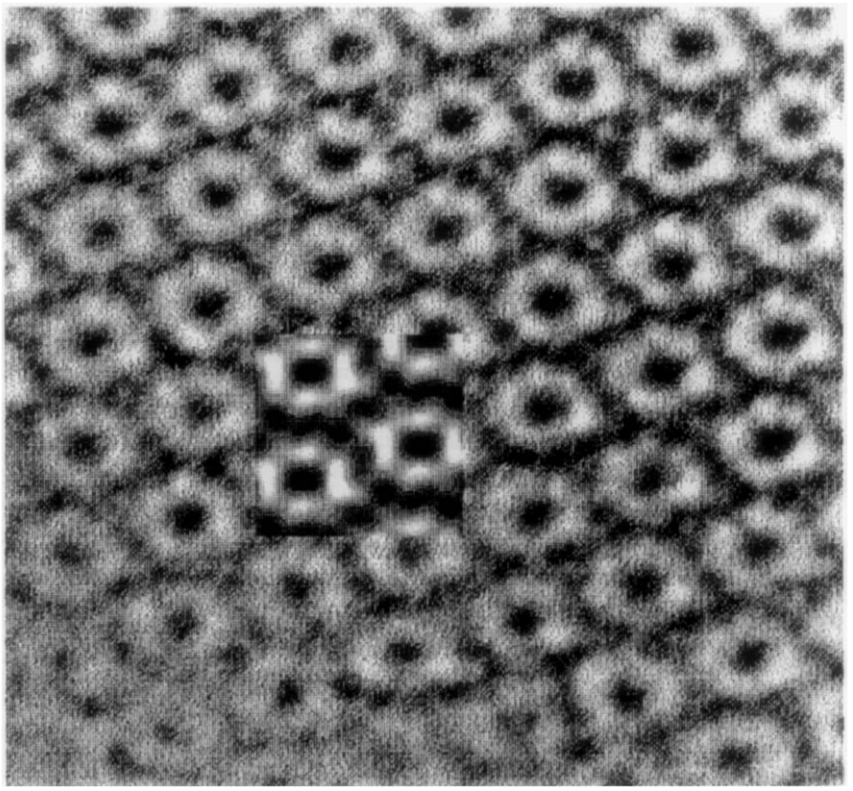

FIG. 10. Enlarged part of Fig. 7 with inserted calculated image. The image was calculated for a thickness of 40 Å and a defocus of −548 Å.

structure is a consequence of the high symmetry of the icosahedron. In the images, spots that are associated with the B_{84} units are seen, also in the rather distorted regions. These units are without doubt stable building blocks in the structure. When discussing the defect structure, however, it seems reasonable to consider a still larger spherical unit, comprising 156 atoms: B_{84} plus the 12 surrounding half-icosahedra (see Fig. 1a). In contrast to the B_{84} element, these units consist of complete icosahedra and are therefore relatively easy to identify in the structure. One such unit can be seen in Fig. 1a as an area centered on $B12_c$, enclosed by a circular ring of low density. In the ordinary boron structure all boron atoms except those belonging to the central $B12_c$ are part of at least two B_{156} units, which are thus interpenetrating. The structural difference between the defect and the normal structure would be possible to describe in terms of B_{156} units as a difference in distance between these larger units. The proposed models for the defects (except IV) discussed in this paper are based on such units. These models leave some space unfilled at the center of the defect, creating possible sites for large atoms such as La.

The boron crystals studied in this investigation are unusually defect-rich and contain new types of defects. Crystals from other samples have been studied, including commercial boron powder and Sc-(*16*) and Cu-doped boron (*17, 18*) and these were found to contain few isolated {100} faults, if any.

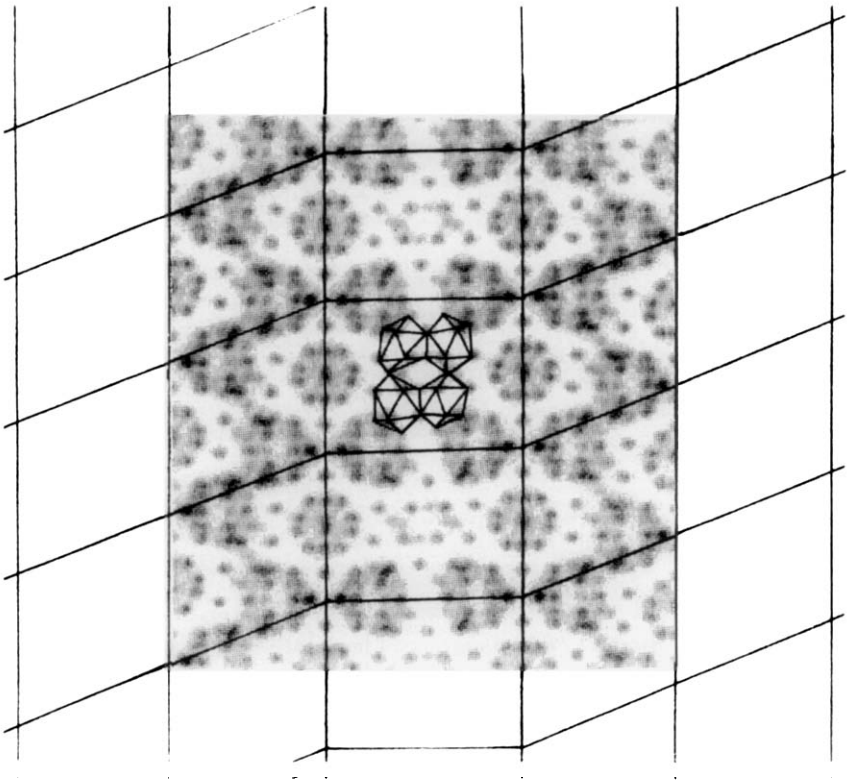

FIG. 11. Projected potential of a model of the defect seen in Fig. 9, with two $B12_6$, $-B12_6$ units indicated. The same projected unit cell as in Fig. 1b is indicated.

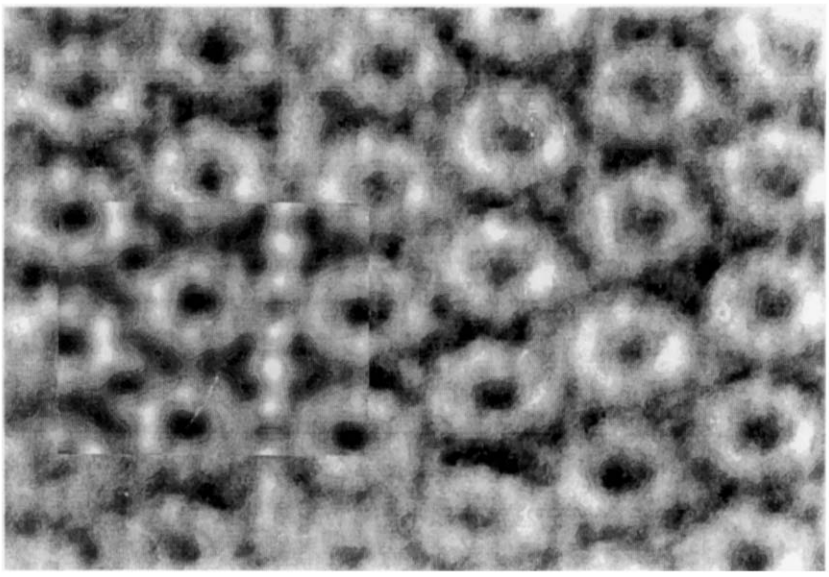

FIG. 12. Part of Fig. 7 with calculated image inserted. The image was calculated for a thickness of 52 Å and a defocus of −622 Å. Images were calculated for this defect using the periodic continuation approach (*14, 15*). Since the unit cell becomes slightly distorted at the short edge of the supercell, only a part of it is used for matching the experimental image. This is not likely to cause any serious change of the simulated image around the defect.

The fact that the analyses indicates that the β-boron crystals from the $La_{0.81}B_6$ sample do contain small amounts of La makes it likely that the defects in the present case are caused by the presence of La.

Acknowledgments

The author thanks Professor Lars Kihlborg for valuable discussions. I am also indebted to Dr. T. Lundström for providing the samples and for his comments on the manuscript.

References

1. T. LUNDSTRÖM, *Z. Anorg. Allg. Chem.* **541/542,** 163 (1986).
2. K. KLEINHENZ AND P. RUNOW, *Phys. Status Solidi* **29,** 627 (1968).
3. H. BINNENBRUCK, A. HAUSEN, P. RUNOW, AND H. WERHEIT, *Z. Naturforsch. A* **25,** 1431 (1970).
4. M. E. ANTADZE, V. N. ROZHANSKII, G. V. TSAGAREISHVILI, AND F. N. TAVADZE, *in* "Bor: Poluchenie, Struktura i Svoista" (F. N. Tavadze, G. V. Samsonov, G. V. Tsagareiskvili, M. E. Antadze, and N. A. Zoidze, Eds.), p. 54, Izdatet-'stuo "Nauka", Moskva (1974).
5. F. N. TAVADZE, G. V. TSAGAREISHVILI, N. A. ZOIDZE, AND M. E. ANTADZE, *in* "Boron" (T. Niemyski, Ed.), Vol. 3, p. 127, Polish Scientific Publications, Warsaw (1970).
6. M. J. MCKELVY, A. R. RAE SMITH, AND L. EYRING, *J. Solid State Chem.* **44,** 374 (1982).
7. R. E. HUGHES, C. H. L. KENNARD, D. B. SULLENGER, H. A. WEAKLIEM, D. E. SANDS, AND J. L. HOARD, *J. Amer. Chem. Soc.* **85,** 361 (1963).
8. J. L. HOARD, D. B. SULLENGER, C. H. L. KENNARD, AND R. E. HUGHES, *J. Solid State Chem.* **1,** 268 (1970).
9. D. GEIST, R. KLOSS, AND H. FOLLNER, *Acta Crystallogr. Sect. B* **26,** 1800 (1970).
10. B. CALLMER, *Acta Crystallogr. Sect. B* **33,** 1951 (1977).
11. YU. PADERNO AND T. LUNDSTRÖM, *Acta Chem. Scand. A* **37,** 609 (1983).
12. M. A. O'KEEFE, *in* "Electron Optical Systems for Microscopy, Microanalysis and Microlitography" (J. J. Hren, F. A. Lenz, E. Munro, and P. B. Sewer, Eds.), Proc. 3rd Pfeffercorn Conf., SEM Inc., AMF O'Hare, IL (1984).
13. M. VLASSE AND J. C. VIALA, *J. Solid State Chem.* **37,** 181 (1981).
14. G. R. GRINTON AND J. M. COWLEY, *Optik* **34,** 221 (1971).
15. S. IIJIMA, *Optik* **47,** 438 (1977).
16. B. CALLMER, *J. Solid State Chem.* **23,** 391 (1978).
17. S. ANDERSON AND B. CALLMER, *J. Solid State Chem.* **10,** 219 (1974).
18. I. HIGASHI, T. SAKURAI, AND T. ATODA, *J. Solid State Chem.* **45,** 283 (1976).